New Phytologist

Research

C_4 photosynthesis and hydraulics in grasses

Haoran Zhou[1], Erol Akçay[2], Erika J. Edwards[3], Che-Ling Ho[2], Adam Abdullahi[2], Yunpu Zheng[4] and Brent R. Helliker[2]

[1]Institute of Surface-Earth System Science, School of Earth System Science, Tianjin University, Tianjin, 300072, China; [2]Department of Biology, University of Pennsylvania, Philadelphia, PA 19104, USA; [3]Department of Ecology and Evolutionary Biology, Yale University, PO Box 208106, New Haven, CT 06520, USA; [4]School of Water Conservancy and Hydropower, Hebei University of Engineering, Handan, 056038, Hebei, China

Author for correspondence:
Haoran Zhou
Email: haoranzhou@tju.edu.cn

Received: *30 July 2024*
Accepted: *30 October 2024*

New Phytologist (2025) **245:** 1481–1495
doi: 10.1111/nph.20284

Key words: A_{max}–K_{leaf}, C_4, grasses, leaf hydraulic conductance, photosynthesis.

Summary

- The anatomical reorganization required for C_4 photosynthesis should also impact plant hydraulics. Most C_4 plants possess large bundle sheath cells and high vein density, which should also lead to higher leaf capacitance and hydraulic conductance (K_{leaf}). Paradoxically, the C_4 pathway reduces water demand and increases water use efficiency, creating a potential mismatch between supply capacity and demand in C_4 plant water relations.
- Here, we use phylogenetic analyses, physiological measurements, and models to examine the reorganization of hydraulics in closely related C_4 and C_3 grasses.
- The evolution of C_4 disrupts the expected positive correlation between maximal assimilation rate (A_{max}) and K_{leaf}, decoupling a canonical relationship between hydraulics and photosynthesis generally observed in vascular plants. Evolutionarily young C_4 lineages have higher K_{leaf}, capacitance, turgor loss point, and lower stomatal conductance than their C_3 relatives. By contrast, species from older C_4 lineages show decreased K_{leaf} and capacitance. The decline of K_{leaf} through the evolution of C_4 lineages was likely controlled by the reduction in outside-xylem hydraulic conductance, for example the reorganization of leaf intercellular airspace.
- These results indicate that, over time, C_4 plants have evolved to optimize hydraulic investments while maintaining the anatomical requirements for the C_4 carbon-concentrating mechanism.

Introduction

C_4 photosynthesis evolved independently >20 times in the grasses over the past 30 million years (Myr) (GPWGII, 2012) as a response to several climatic variables, each of which increased photorespiration in C_3 progenitors. The C_4 photosynthetic pathway increases the efficiency of photosynthesis by creating a carbon concentrating mechanism (CCM) around the enzyme Rubisco, hence reducing the oxygenase activity of Rubisco and photorespiration. Multiple environmental drivers interacted throughout this evolutionary timeline (Zhou *et al.*, 2018), and while the high temperature was a persistent selective pressure, water availability likely drove the evolution of the earliest C_4 lineages (Edwards & Smith, 2010; Sage *et al.*, 2018; Zhou *et al.*, 2018). Low atmospheric CO_2 was the strongest environmental driver of C_4 evolution and distribution within the last 10 Myr (Ehleringer & Monson, 1993; Ehleringer *et al.*, 1997). Regardless of the primary selective driver, each separate evolutionary event required significant anatomical changes and biochemical reorganization within a grass blade to achieve a fully functional C_4 CCM (Griffiths *et al.*, 2012; Osborne & Sack, 2012; Sage *et al.*, 2012; Edwards, 2019; Leakey *et al.*, 2019; Schlüter & Weber, 2020). Anatomical changes include increased vein density (decreased interveinal distance (IVD)) and increased bundle sheath size, which lead to high bundle sheath-to-mesophyll ratios. The biochemical reorganization includes sequestration of the Calvin–Benson within the bundle sheath cells and upregulation of PEP carboxylase as the primary carboxylation enzyme in the mesophyll cells, as well as increased carbonic anhydrase activity. These modifications were necessary for optimal operation of C_4 photosynthesis but also likely affected plant water relations.

Compared with measurements of water loss during photosynthesis, there has been little focus on how the evolution of the C_4 CCM impacted grass water relations, in particular, leaf hydraulics and hydraulics–photosynthesis relationships (Edwards, 2019; Leakey *et al.*, 2019; Schlüter & Weber, 2020; Vadez *et al.*, 2021). C_4 plants typically exhibit lower stomatal conductance and consequently greater water use efficiency than C_3 plants under similar environmental conditions, because of the high affinity for CO_2 of PEP carboxylase, permit a high assimilation rate at reduced intercellular CO_2 concentrations and more conservative stomatal behavior (Pearcy & Ehleringer, 1984; Huxman & Monson, 2003; Way *et al.*, 2014). This enhanced water use efficiency is thought to be behind C_4 grasses being found in drier environments than C_3 grasses when controlling for

phylogeny (Edwards & Still, 2008; Pau *et al.*, 2013). The focus on stomatal conductance is important to assess the balance of carbon gain to water loss, but the supply side – the movement of water through leaf veins and ultimately to stomata – is where the requisite anatomical changes inherent to C_4 grasses, such as increased vein density and increased bundle sheath size could yield a substantial impact on water relations and hydraulics–photosynthesis relationships.

The anatomical requirements for C_4 evolution and the higher water use efficiency associated with the CCM lead to an ecophysiological paradox. C_4 plants require high bundle sheath-to-mesophyll ratios, which are accomplished with increased vein density and bundle sheath size. Decreased IVD and larger xylem diameter in C_4 grasses (Ueno *et al.*, 2006; Hamim *et al.*, 2016) are predicted to lead to a higher leaf hydraulic conductance (K_{leaf}) in C_4 grasses as compared to closely related C_3 grasses (Griffiths *et al.*, 2012; Osborne & Sack, 2012). Such predictions emanate from the generally observed positive relationship of K_{leaf} with vein density observed broadly in C_3 species (Sack & Frole, 2006; Brodribb *et al.*, 2007; McKown *et al.*, 2010; Scoffoni *et al.*, 2016). Furthermore, increased bundle sheath size is proposed to result in higher leaf capacitance, or water storage, in C_4 species (Sage, 2001; Griffiths *et al.*, 2012). The combination of the C_4 CCM with increased vein density and bundle sheath size therefore creates a 'hydraulic paradox', consisting of a photosynthetic pathway that should simultaneously increase supply-side hydraulic capacity while reducing transpiration demand.

With over 20 origins of C_4 photosynthesis with ages that span *c.* 30 Myr, grasses also present a unique opportunity to examine the influence of C_4 evolution on the relationship between photosynthesis and water transport. Maximum photosynthetic rate (A_{max}) and leaf hydraulic capacity (K_{leaf}) have been shown to be tightly linked in C_3 plants. The ability to transport water through leaves to the sites of evaporation at a high rate enables greater stomatal conductance for a given vapor pressure deficit (VPD), and results in a higher leaf water potential which improves the biochemical efficiency for the maximization of carbon gain (Brodribb & Field, 2000; Brodribb *et al.*, 2005, 2007; Sack & Frole, 2006; Fiorin *et al.*, 2016). Indeed, a strong, positive correlation between A_{max} and K_{leaf} was detected across a broad phylogenetic spectrum of species spanning vascular plants (Brodribb *et al.*, 2007). Within a clade of closely related eudicot species with the C_3 photosynthetic pathway, maximizing K_{leaf} was found to be a 'fundamental requirement' to increasing A_{max} (Scoffoni *et al.*, 2016). Within C_4 grasses, there is a suggestion that the A_{max}–K_{leaf} relationship does not hold (Ocheltree *et al.*, 2016; Pathare *et al.*, 2020), but these studies did not examine closely related C_4 and C_3 grasses. C_4 origins are not distributed uniformly across plant lineages, but are clustered in the specific 'PACMAD' clade (Edwards & Smith, 2010; Christin *et al.*, 2013). Any physiological differences between distantly related C_3 and C_4 species could result from differences in selective pressures and/or evolutionary trajectories within a specific clade having little to do specifically with photosynthetic pathway variation (Donnelly *et al.*, 2023). Thus, in order to establish the specific impact of C_4 evolution on the relationship between K_{leaf} and A_{max}, phylogenetically informed studies considering closely related C_3 and C_4 grasses are necessary (Edwards & Still, 2008; Edwards & Smith, 2010).

In this study, we address two broad hypotheses. First, we hypothesize that the enhanced vein density and bundle sheath size in C_4 grasses leads to greater water supply irrespective of the decreased water demand that the C_4 CCM imparts. Second, we predict that the hydraulic paradox of increased supply with decreased stomatal conductance of the C_4 pathway disrupted the expected relationship between water supply through the leaf (K_{leaf}) and maximum photosynthesis (A_{max}). We examine these hypotheses within an evolutionary framework by using closely related clusters of C_3 and C_4 grasses (Fig. 1, Supporting Information Figs S1, S2). We determined whether anatomical differences associated with C_4 evolution result in greater K_{leaf}, leaf capacitance, and turgor loss points compared with their C_3 relatives through examining whether there were different evolutionary stable states between C_3 and C_4 in the best-fitted evolutionary model. We then determined whether C_4 evolution alters predicted A_{max}–K_{leaf} relationships. Finally, we examined evolutionary trends in K_{leaf}, capacitance, and leaf turgor loss point after the evolution of C_4 within a lineage by asking whether more recent origins of C_4 are represented by directional changes in hydraulics and a greater K_{leaf}–A_{max} mismatch.

Materials and Methods

Plant materials

We collected seeds of closely related C_3 (9 species) and C_4 species (29 species), representing three C_4 subtypes, nine C_4 origins, and one C_3–C_4 intermediate species (however, we did not include the intermediate species in the phylogenetic comparative methods). All species are amphistomatous. The selected C_3 and C_4 species fall into nine identified C_4 lineages out of the 24 grass lineages (11 out of the 24 have clear C_3 sister species and the 11 lineages are recommended for comparative studies in GPWGII, 2012): *Aristida*, *Stipagrostis*, *Chloridoideae* (*Eragrostideae*), *Eriachne*, *Tristachyideae*, *Arthropogoninae*, *Otachyrinae* (*Anthaenantia*), *Panicinae*, *Melinidinae* and *Cenchrinae* (Fig. 1). C_3 and C_4 species numbers cannot be totally balanced due to the rarity of closely related C_3 species in the lineages we sampled. However, the among lineage coverage is nonetheless expected to give good power to estimate our trait evolution model. In 2015, seeds were surface sterilized before germination and the seedlings were transferred to 15 cm, 1.49 l pots with Fafard #52 soil (Sungro, Ajawam, MA, USA). Six replicates of each species were randomized in the glasshouse of the University of Pennsylvania supplemented with artificial lighting. The plants were watered twice daily. Day : night temperatures ranged from 23.9 to 29.4 : 18.3 to 23.8°C, and relative humidity from 50% to 70%. Plants were fertilized once per week with 300 ppm nitrogen solution (Jacks Fertilizer; JR Peters, Allentown, PA, USA), and 0.5 tsp of 18–6-8 slow-release Nutricote Total (Arysta Life Science America Inc., New York, NY, USA), was applied per pot upon transference to pots. To maintain optimal plant growth a 15-5-

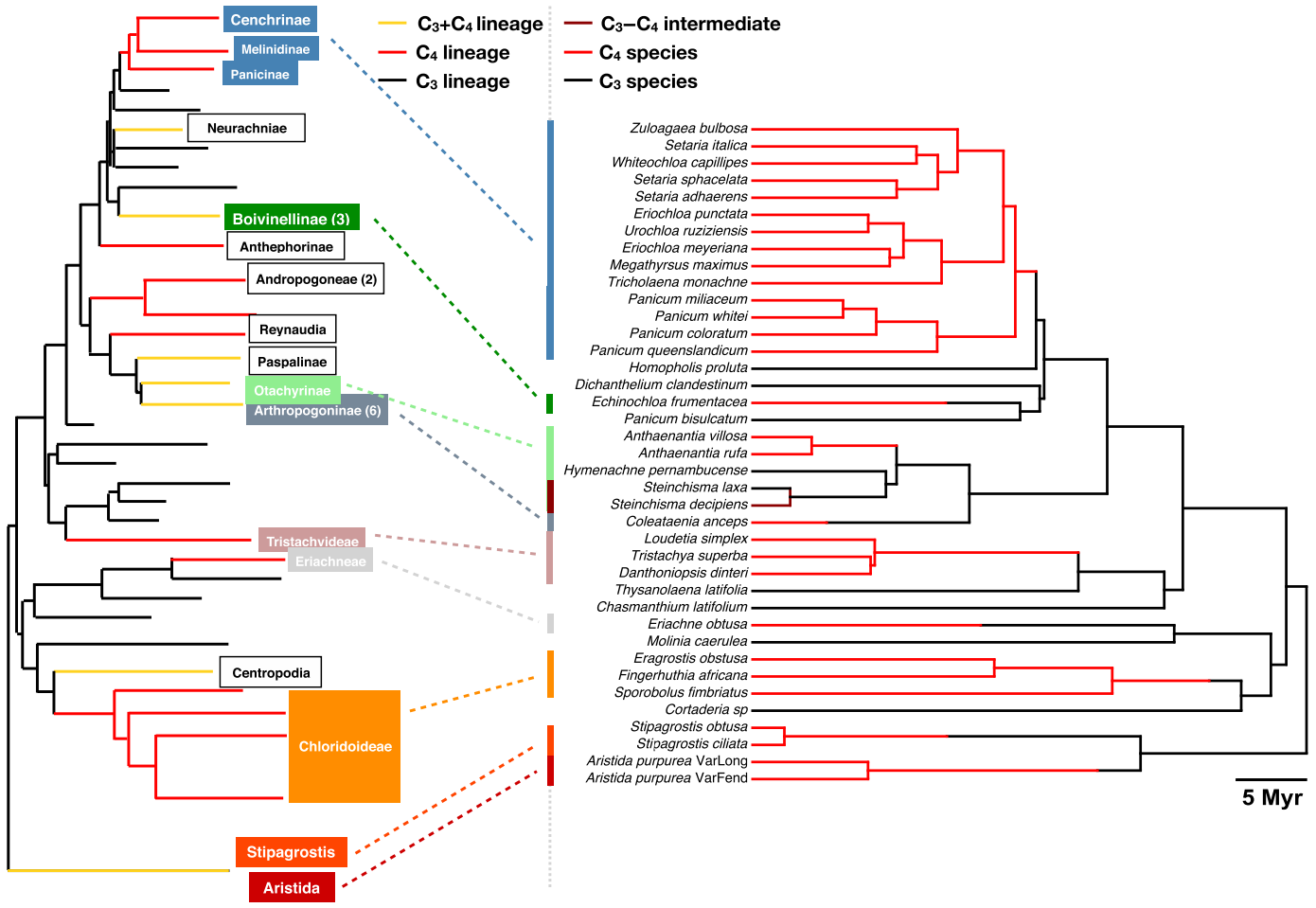

Fig. 1 Phylogenetic sampling of the species for measuring physiological traits and the independent evolutionary lineages corresponding to grass lineages. The figure on the left is a nondated grass phylogeny adapted from GPWGII (2012), on which the tags represent the recommended independent evolution of C_4 for comparative studies in grasses (numbers represent multiple origins within a lineage). The figure on the right is the phylogeny for the species sampled in our experiments, extracted from a dated phylogeny (Spriggs *et al*., 2014). We sampled nine independent evolutions of C_4 in total. We used different colors to indicate different lineages. Red branch length indicates C_4, black branch indicates C_3, and brown branch indicates one intermediate species of *Steinchisma decipiens* Nees ex Trin.

15 cal-mg fertilizer was used every third week. All measurements were performed on the most recent fully expanded leaves to ensure they all grew under similar environmental conditions.

Physiological measurements

Leaf hydraulic conductance (K_{leaf}) was measured using the evaporative flux method (Sack & Scoffoni, 2012), with some adjustments to maintain the stability of the evaporative environment to which the leaf was exposed, using a custom-built, environmentally controlled cuvette. The evening before measurements, potted plants were brought to the laboratory, well-watered, and then covered by black plastic bags filled with wet paper towels to rehydrate overnight. The most recent fully expanded leaves from each plant were used for K_{leaf} measurements. For the leaf gasket, a 1 cm diameter, *c*. 1 cm long solid silicone rubber cylinder was cut nearly in two, leaving a hinge on one end. The cylinder was placed around the leaf blade near the ligule and glued shut with superglue (T. Ocheltree, pers. comm.). The leaf was cut from the plant with a razor blade while submerged in a 15 mmol l^{-1} KCl solution; the rubber gasket was then attached to tubing filled with the same KCl solution. The other end of the tubing was inside a graduated cylinder that sat on a digital balance (Mettler Toledo, OH, USA). The leaf was then placed inside a custom, environmentally controlled cuvette that allowed for the measurement of entire grass blades. The cylindrical glass cuvette is 50 cm long with a 6 cm diameter. It was surrounded by a second glass cylinder that was sealed off with the exception of two nozzles that allowed for the circulation of temperature-controlled water. Within the cuvette, the leaf rested on a 48 cm long, removable threaded-rod insert that had attached to it: 11 air-stirring fans; a leaf thermocouple; a shielded temperature/relative humidity sensor (Sensirion SHT75, IL, USA); and tubing for incoming/outgoing air supply. Chamber air was first pulled from tubing attached to a rooftop sample port and then passed to two 20-l carboys in series, and then into the pump

intake. Air was then pushed from the diaphragm pump (Brailsford, Antrim, NH, USA) to a heated water bubbler to saturate the air and onto a water-jacketed glass coil that was temperature controlled at the desired dew-point temperature. Air then passed to a mass flow controller (MKS) set at 2 l m^{-1} and to a second mass flow meter (Sierra Instruments, CA, USA) and into the cuvette. A sodium-halide lamp was positioned directly above the chamber. Photosynthetically active radiation in the system was 1000 μmol m^{-2} s^{-1}. Throughout measurements, cuvette temperature was controlled at 25°C and the humidity was 55–65% (VPD range of 1.1–1.4 kPa) across measurements, but remained constant during a particular measurement. Flow from the balance was monitored for 45 min to 1 h until the flow rates reached a steady state (Sack & Scoffoni, 2012). After the measurements, the leaf was detached and was put into a plastic bag to equilibrate for 20 min. After equilibration, leaf water potential was measured using a pressure chamber (Model 1000; PMS Instrument, OR, USA). Leaf area was determined by using a digital photograph and ImageJ. K_{leaf} values were further standardized to 25°C to make the K_{leaf} comparable among studies and across species. Data indicating a sudden change in flow and whose leaf water potential was an obvious outlier were deleted.

Theoretical xylem hydraulic conductance (K_x) was measured on a subset of five species to compare with K_x derived from anatomical measurements. The empirical determination of K_x follows the method of Stiller *et al.* (2003). Similar to K_{leaf} measurements, a rubber gasket was attached to the leaf blade while still attached to the plant, and the leaf was excised under water. The gasket was joined to a tubing system connected to a water-filled glass flask that can be lowered *c.* 50 cm to generate a pressure gradient. The leaf was cut a second time at its widest point, closer to the mid-leaf typically yielding a 2–3 cm leaf section. By using the widest part of the leaf, we avoided vessel narrowing to obtain maximum flow. The cut tip was submerged, just below the meniscus, in a small water-filled graduated cylinder placed on an electronic balance (Mettler Toledo). To create a pressure gradient, the flask supplying the water to the leaf was lifted to different heights and maintained at each height until a steady-state flow was achieved. K_x was calculated from linear regression between flow rate and the gravity-induced pressure. K_x was normalized by leaf area. After measurements, the leaves were flushed at *c.* 100 kPa with water to check for continuous aerenchyma. If bubbles appeared, the measurement was discarded.

We measured pressure–volume (PV) curves for six leaves per species using the bench-drying method (Tyree & Hammel, 1972; Sack & Pasquet-Kok, 2010). A leaf was cut directly from the same plants rehydrated in the laboratory (as mentioned in the previous section) using a razor blade and leaf water potential was measured immediately, and leaf mass subsequently recorded. The leaf was initially allowed to dry on the bench for 2-min intervals and put into a ziplock bag and under darkness for 10-min equilibration before measuring the leaf water potential and mass again. The length of subsequent intervals was adjusted based on the decrease in the leaf water potential (from 2 min to 1 h) to obtain an approximate decreasing gradient of −0.2 MPa per measurement until the leaf mass reached a steady state. At the end of the experiment, leaves were dried in the oven at 70°C for 48 h to obtain the dry mass. The PV curves were used in curve fitting to obtain leaf capacitance (absolute capacitance per leaf area at full turgor), and leaf turgor loss point using an Excel program from Sack and Pasquet-Kok (2010).

Maximal assimilation rates (A_{max}) were obtained through a light curve similar to Brodribb *et al.* (2007). A_{max} and stomatal conductance measurements were obtained using a standard 2 × 3 cm^2 leaf chamber with a red/blue LED light source of LI-6400XT (LI-COR Inc., Lincoln, NE, USA). Light curves were measured with light intensities of 2000, 1500, 1200, 1000, 800, 500, 300, 200, 150, 100, 75, 50, 20, and 0 μmol m^{-2} s^{-1} under reference CO_2 of 400 ppm (to represent the atmospheric CO_2) with a controlled VPD of 1 kPa in the leaf chamber. Then, A_{max} was estimated from the light curve (Marshall & Biscoe, 1980). Controlling reference CO_2 instead of sample CO_2 may affect the light curves, but we found the average difference between reference and sample CO_2 to be 1.28% in our study, which had little impact on our results (Table S1). Together with the measurement, corresponding g_s was measured. All the measurements were made under the temperature of 25°C. g_s at the saturated light intensity of 2000 μmol m^{-2} s^{-1} was recorded for each plant. The cuvette opening was covered by putty to avoid and correct for leakiness.

Anatomical measurements

One fully expanded leaf of each replicate ($n = 6$) was used for measuring leaf anatomy. All the images were taken under a light microscope with a mounted camera (Nikon D300, Japan) and the digCamControl software. A *c.* 1 mm free-hand cross-section was made, and IVD (μm) and mid-rib xylem diameter (μm) and bundle sheath cross-sectional area were measured using these images. A 4-mm-long section from the same leaf blade was cut and submerged in 10% bleach solution until transparent for vein density (mm mm^{-2}) and bundle sheath measurement. For bundle sheath area, we measured the inner bundle sheath distance, which is from the inside edge of the bundle sheath cells, and the outer bundle sheath distance, which is from the outer edge of the bundle sheath cells on either side of each bundle, for each vascular bundle. Then, we used the outer bundle sheath distance minus the inner bundle sheath distance, and multiplied them with the vein length per leaf area. Anatomical measurements were calculated using Fiji (Schindelin *et al.*, 2012). Intercellular air space (IAS, %) was measured according to Males & Griffiths (2018) and Smith & Heuer (1981). In brief, one leaf from each of the rehydrated plants was cut and placed in ziploc bag with wet paper towels for 30-min equilibration and followed by whole-leaf water potential (MPa) measurement. The leaf blade was cut into 1 cm × 4 mm slices, weighed, and placed into a Petri dish with isotonic mannitol solution. Samples were vacuumed for 15–20 s until reaching −26 MPa. Ambient air was then slowly brought in. The slices were dabbed dry and weighed again for postinfiltration mass (g). Vacuum and weighing processes were repeated until no mass change was observed. IAS was calculated as the ratio of sample mass change to maximum postinfiltration mass.

We measured xylem conduit diameters to calculate K_x using the Hagen–Poiseuille equation (Scoffoni *et al.*, 2011; North *et al.*, 2013). For each leaf sample, digital photographs from the leaf edge to the mid-rib (or the other edge if possible) were taken sequentially with a microscope (West Germany) connected to a Nikon D3300 digital camera (Japan) and DigiCamControl program. To minimize over-estimation of K_x by simply using mid-rib conduit diameter values, the meta-xylem conduit diameter of the mid-rib and outermost major vein on each side (three major veins in total) was measured with FIJI (IMAGEJ, USA) elliptical selection tool. If the leaf cross-section only contained half of the leaf blade, the outermost major vein was doubled in the calculation. The Hagen–Poiseuille equation for each conduit was chosen according to the shape of the conduit (Lewis, 1992; Lewis & Boose, 1995) determined by the ratio of the elliptical long to short axes (> 1.1 is an ellipse, otherwise a circle). The Hagen–Poiseuille equation for ellipse conduit,

$$K_{\text{conduit}} = \frac{\pi a^3 b^3}{64\eta\left(a^2 + b^2\right)}$$

where a and b are the elliptical axes and η is the viscosity of water at 25°C. For the circle conduit, the diameter (d) was calculated as the average of axes, and

$$K_{\text{conduit}} = \frac{\pi d^4}{128\eta}$$

After adding up the K_{conduit} for each vein, the average of the three veins was calculated to present the hydraulic conductance of the major vein of the sample (K_{major}, $\text{m}^4\,\text{MPa}^{-1}\,\text{s}^{-1}$), and the total major vein hydraulic conductance was calculated as the K_{major} multiplied by the number of major veins. The outcome was further normalized by leaf area (m^2) and leaf length (m) to convert to K_x with the unit $\text{mmol}\ \text{m}^{-2}\,\text{s}^{-1}\,\text{MPa}^{-1}$ (North *et al.*, 2013). Anatomy-based K_x values were compared with measured values of K_x on a subset of five species (Fig. S3).

After obtaining the xylem hydraulic conductance value, we further calculated the outside-xylem hydraulic conductance (K_{ox}). We calculate K_{ox} using the K_{leaf} and K_x using the following equation,

$$\frac{1}{K_{\text{leaf}}} = \frac{1}{K_x} + \frac{1}{K_{ox}}$$

Phylogenetic comparative analysis

We extracted the nondated and dated phylogeny from published grass phylogenies to include only the target species in our physiological experiments (GPWGII, 2012; Spriggs *et al.*, 2014; Figs 1, S1, S2). Branches of the extracted phylogenies retained classifications as C_3 or C_4 in the original trees. We performed the following analyses for the two phylogenies to make sure the analyses were not biased by different ages by using the dated tree, nor different rates of evolution across lineages by using the nondated tree. Using both of the phylogenies, for each of the hydraulic traits, we fitted evolutionary models to test which model best explains the observed distribution of traits along the phylogeny and how these models differ between C_3 and C_4 using 'mvMORPH' in R (Clavel *et al.*, 2015; Tables 1, S2). We fitted evolutionary models belonging to Brownian motion-type models and Ornstein–Uhlenbeck-type models. The evolutionary models have nested variants (Models 1–4; Models 5–6), varying in whether C_3 and C_4 species had the same or different drift rates, and root states. To determine the best-fitted evolutionary model, we used two criteria: the small-sample-size corrected version of Akaike information criterion (AICc, the lower AICc, the better fit) and Akaike weights (AICw, the higher AICw, the better fit; Akaike, 1974; Cavanaugh, 1997; Burnham & Anderson, 1998). We used likelihood-ratio test (LRT) to verify whether a specific model variant performs significantly better. The AICc, AICw, and LRT allowed us to test evolutionary hypotheses, for instance, if the model in which C_3 and C_4 have different root states fit significantly better than model in which C_3 and C_4 have the same root states, it means there was a shift of a given physiological trait along with the formation of C_4. To further test whether there are significant differences among C_4 subtypes, evolutionary models with subtypes (Methods S1; Table S3) were used to fit the data.

Table 1 Evolutionary models used for the phylogenetic analysis for hydraulic and photosynthetic traits to test evolutionary differences between C_3 and C_4 species.

Model	Evolution	Drift rate	Root
Model 1	BM1	One	One
Model 2	BM1	Two	One
Model 3	BM2	One	Two
Model 4	BM2	Two	Two
Model 5	OU1	One	One
Model 6	OU2	One	Two

To examine the further evolution of hydraulic traits after the evolution of a full C_4, we extracted the evolutionary ages/branch lengths for each represented C_4 origin from both phylogenetic trees. Then, we regressed the traits with evolutionary age. A significant negative correlation between evolutionary age and hydraulic trait indicates a further directional change after C_4 evolved. We used the Benjamini–Hochberg method to control the overall false discovery rate and calculate the adjusted P-values. In addition, the nondated phylogeny allowed us to fit for an additional six Brownian motion models with trend (Table S2). Likewise, if the Brownian motion model with trend fitted the phylogenetic patterns better than the Brownian motion model without trend, it would mean there is an evolutionary trend, and a significant LRT test for a two-trend model suggests that C_3 and C_4 lineages differ in the speed or direction of trait evolution.

Multivariate analysis in 'mvMORPH' was used to estimate the correlations between A_{max} and each of the hydraulic traits and between K_{leaf} and anatomical traits to test the hypotheses that anatomical differences associated with C_4 evolution result in greater K_{leaf} and result in significantly different correlations between C_3 and C_4. Seven different correlation models were fitted (Table 2). Such correlation analysis is similar to

Table 2 Description of the models for correlation between maximal assimilation rate (A_{max}) and physiological traits.

General model	Type	Model description
CorModel 0	No correlation	Null model: no correlation between traits in C_3 and C_4
CorModel 1	Variance & Covariance	C_3 and C_4 shared variance and covariance for two traits
CorModel 2	Proportional	C_3 and C_4 have proportional variance and covariance matrix
CorModel 3	Eigenvector	C_3 and C_4 shared direction and pattern for variance and covariance matrix
CorModel 4	Correlation	C_3 and C_4 shared correlation for two traits
CorModel 5	Variance	C_3 and C_4 shared variance for two traits
CorModel 6	C_3 C_4 independent	C_3 and C_4 have independent variance and covariance matrix

phylogenetic generalized least squares considering C_3 and C_4, but with more varieties on the setting of variance and covariance matrix. The small-sample-size corrected version of Akaike information criterion (AICc, the lower AICc, the better fit) and Akaike weights (AICw, the higher AICw, the better fit; Akaike, 1974; Cavanaugh, 1997; Burnham & Anderson, 1998) and LRT were used to identify the best-fitted model and test whether the correlation of the two traits is significantly different from 0, and whether the correlation of two traits is significantly different between C_3 and C_4 in the above analyses.

Physiological modeling

We used our previously constructed C_3 and C_4 physiological models (Zhou *et al.*, 2018; https://github.com/zhouhaoran06), that coupled the photosynthesis systems and hydraulic systems, to predict the effect of changing K_{leaf} on the assimilation rate (Table S4). The model incorporates the soil–plant–air–water continuum into C_3 and C_4 photosynthesis models and assumes that plants optimize stomatal resistance and leaf/fine-root allocation to balance carbon gain and water loss. We considered that for plant hydraulic transportation under an equilibrium state, the rate of water loss through transpiration should balance the rate of root absorption. We modeled assimilation rates of C_3 and C_4 under different CO_2 concentrations, water limitation conditions, and temperatures. The change in measured K_{leaf} was assumed to change the modeled plant hydraulic conductance (K_{plant}) proportionally in the modeling process, as K_{plant} scales with the K_{leaf} (Sack *et al.*, 2003; Sack & Holbrook, 2006; Wolfe *et al.*, 2022) and K_{leaf} is generally the bottleneck for conductance through the plant (Sack *et al.*, 2003). Furthermore, grass K_{root} is four (C_4 grasses) to nine times (C_3 grasses) higher than K_{leaf} (Ocheltree *et al.*, 2014). We analyzed the effects of varying K_{leaf} on assimilation rates for C_3 and C_4 grasses using the model, specifically through doubling K_{leaf} or reducing K_{leaf} by half relative to the original value and modeling the corresponding photosynthesis rates.

Results

Analyzing our data using the evolutionary models listed in Table 1 revealed significant C_3–C_4 differences in most measured traits, including K_{leaf}, stomatal conductance, turgor loss point, and A_{max} (Fig. 2; Table 3). We first fitted evolutionary models of Brownian motion and Ornstein–Uhlenbeck processes to the measured physiological traits based on a reliable dated phylogenetic tree (Spriggs *et al.*, 2014) and identified the best-fitted models (Tables 3, S5–S9). Different theta (Ornstein–Uhlenbeck model) or root (Brownian motion model) values in the best-fitted models indicate a significant difference for C_3 and C_4 grasses. C_4 grasses had higher K_{leaf} and A_{max}, less-negative turgor loss point, and lower stomatal conductance as compared to C_3 grasses (LRT test, all $P < 0.01$; all $\Delta AICc < -3$; Table 3; Fig. S4). For leaf capacitance, there was no significant difference for C_3 and C_4 grasses. Additionally, we found no significant differences in K_{leaf}, leaf capacitance, g_s, leaf turgor loss point, and A_{max} among C_4 subtypes (Tables S3, S10; Notes S1).

We next explored how A_{max} and hydraulic traits, and K_{leaf} and anatomical traits, are correlated across the phylogeny using the models listed in Table 2, and whether this relationship is different for C_3 and C_4 grasses (Tables 4, S11–S20). For C_3 grasses, we found expected relationships as A_{max} was positively correlated with K_{leaf} (Table 4; Fig. 2). Leaf anatomical controls on the efficiency of water movement also was congruent with previous research, as we found a positive correlation between vein density and K_{leaf} (and a correspondingly negative correlation between IVD and K_{leaf}) and a positive relationship between K_{leaf} and intercellular air space in C_3 species (Table 4; Fig. 2). By contrast, there was no relationship between K_{leaf} and A_{max} in C_4 grasses, nor was there any relationship between K_{leaf} and vein anatomy or intercellular air space or conduit diameter (Table 4; Fig. 2). A_{max} was positively correlated with stomatal conductance and leaf capacitance, and the correlations were not significantly different for C_3 and C_4, while no significant correlation between A_{max} and leaf turgor loss point/bundle sheath size and between K_{leaf} and conduit diameter/bundle sheath size, was found in either C_3 and C_4 (Table 4; Fig. 2).

We also looked for evolutionary trends in hydraulic traits after the evolution of C_4 to probe for an extended 'optimization' phase of C_4 evolution (Edwards, 2019; Heyduk *et al.*, 2019). Identifying directional trends in continuous character evolution is difficult without fossil taxa; however, we can test for trends indirectly using extant species. For example, if maintaining a higher K_{leaf} than is required is maladaptive, selection would reduce K_{leaf} over time in C_4 lineages, and we might expect older C_4 lineages to have lower K_{leaf} values than younger C_4 lineages. We extracted the evolutionary age of C_4 origin for each of our lineages from the dated phylogeny and branch length from a nondated phylogeny (which include both information of relative evolutionary age and different substitution rates across lineages). Regressions of evolutionary age vs hydraulic traits provide evidence for a long-term directional trend in hydraulic evolution following the origin of C_4 photosynthesis (Figs 3, S5). K_{leaf}, turgor loss point, and capacitance showed significant negative correlations with

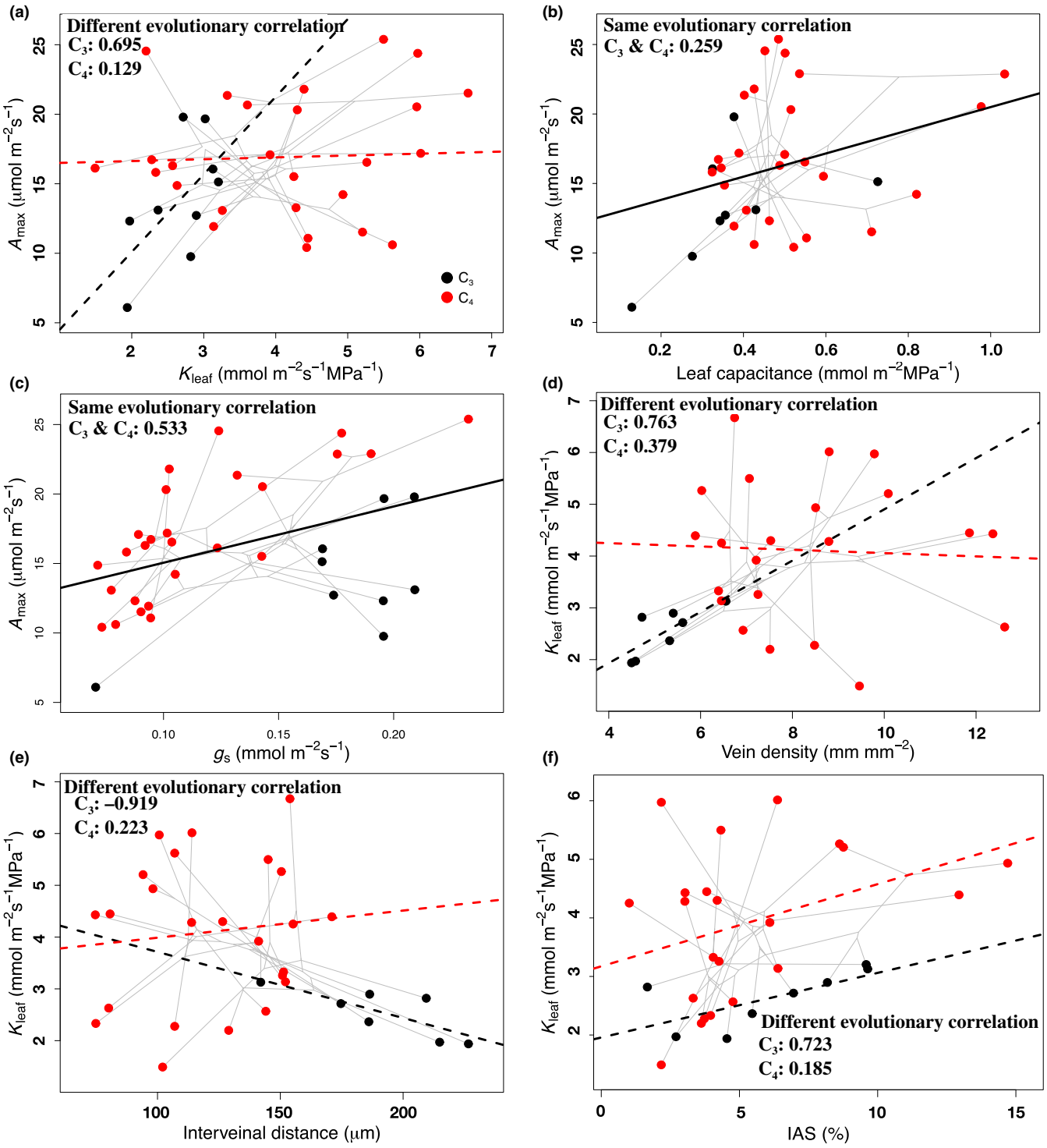

Fig. 2 Phylogenetic correlation for C_3 and C_4 between A_{max} and other hydraulic traits and between leaf hydraulic conductance (K_{leaf}) and anatomical traits. Phylogenetic correlations are (a) K_{leaf}-A_{max}, (b) leaf capacitance-A_{max}, (c) g_s-A_{max}, (d) vein density-K_{leaf}, (e) interveinal distance-K_{leaf}, and (f) intercellular airspace (IAS)-K_{leaf}. Dashed black line: correlation line for C_3; dashed red line: correlation line for C_4; solid black line: C_3 and C_4 have the same correlation and the line shows the same correlation line; grey lines indicate the phylogeny. Different/same correlation values on the figure mean C_3 and C_4 have significantly different/same correlations. Detailed phylogenetic correlation models and analysis results are shown in Table 4. The C_3–C_4 intermediate species was not included in our phylogenetic comparative analyses.

evolutionary age, while A_{max} had a significant positive correlation. By contrast, there was no significant relationship between stomatal conductance and evolutionary age. No evolutionary relationships were detected in C_3 species, which indicated the correlations between evolutionary age and hydraulic traits were unique to C_4 species. In a second approach, we also tested for

New Phytologist

Table 3 Phylogenetic comparative results of hydraulic and photosynthetic traits.

Property	Model	Model type	AICw	Root/Theta	
				C_3	C_4
K_{leaf}	Model 6[a]	OU2	0.984	2.682	4.295
Capacitance	Model 2	BM1	0.323	0.523	
g_s	Model 6[a]	OU2	0.980	0.183	0.102
Turgor loss	Model 6[a]	OU2	0.996	−1.522	−1.192
A_{max}	Model 6[a]	OU2	0.5292	13.66	17.34

Results of the best-fitted models and their parameters for hydraulic conductance (K_{leaf}), leaf capacitance (Capacitance), stomatal conductance (g_s), and leaf turgor loss point (Turgor loss) using the dated phylogeny (summarizing Supporting Information Tables S5–S9). Different root or theta values indicate that the evolutionary model for C_3 and C_4 species is a significantly better fit than the evolutionary model with the same root or theta. Model 6 represents a model following the Ornstein–Uhlenbeck evolutionary process with different evolutionary stable states following (OU2); Model 2 represents a model following the Brownian Motion evolutionary process with a similar evolutionary root state (BM1). Detailed model description can be found in Table 1.
[a]Model fit significantly better than all the other models.

Table 4 Phylogenetic correlations between photosynthetic, hydraulic, and anatomical traits.

Parameter 1	Parameter 2	Best model	r for C_3	r for C_4	*P*-value
A_{max}	K_{leaf}	CorModel 3	0.695	0.129	0.012/0.51
A_{max}	Capacitance	CorModel 2	0.259		0.027
A_{max}	g_s	CorModel 1	0.533		0.003
A_{max}	Leaf turgor loss	CorModel 1	−0.223		0.256
A_{max}	Bundle sheath size	CorModel 1	0.428		0.582
K_{leaf}	Vein density	CorModel 3	0.763	0.379	0.042/0.836
K_{leaf}	Interveinal distance	CorModel 3	−0.919	0.223	0.038/0.608
K_{leaf}	IAS	CorModel 3	0.723	0.185	0.063/0.100
K_{leaf}	Conduit diameter	CorModel 0	NA	NA	NA
K_{leaf}	Bundle sheath size	CorModel 0	NA	NA	NA

Correlation between maximal assimilation rates (A_{max}) and hydraulic traits (K_{leaf}, capacitance, and g_s) and between K_{leaf} and anatomical traits (vein density/interveinal distance/IAS/conduit diameter/bundle sheath size) for C_3 and C_4 species using the dated phylogeny (summarizing Supporting Information Tables S11–S20). Different r means the best-fitted model assuming different correlations for C_3 and C_4. One r means the best-fitted model assuming similar correlations for C_3 and C_4. *P*-values indicate whether the correlation coefficients are significant. NA means that the parameter not applied for the model. CorModel 0 represents a phylogenetic correlation model assuming that there is no correlation between two traits in C_3 and C_4 species; CorModel 1 represents a phylogenetic correlation model assuming that C_3 and C_4 shared variances, covariances and correlations for two traits; CorModel 2 represents a phylogenetic correlation model assuming that C_3 and C_4 have proportional variance, covariance matrix and similar correlations for two traits; CorModel 3 represents a phylogenetic correlation model assuming that C_3 and C_4 shared eigenvector for variance and covariance, and but have different correlations for two traits. Detailed model descriptions could be found in Table 2.

evolutionary trends by modeling hydraulic trait evolution using a phylogeny with branch lengths scaled to molecular substitutions/sites, which provides an estimate of differences in evolutionary rates between lineages (GPWGII, 2012) through fitting 12 different types of models with or without evolutionary trends (Tables S2, S21–S26). While the second approach requires many assumptions that are likely violated, the results also provide additional support to a directional trend in K_{leaf}, capacitance, A_{max} and turgor loss point in C_4 lineages, but no significant directional trend in stomatal conductance.

To estimate anatomical controls on K_{leaf} through evolutionary time, we examined the two controls on K_{leaf}: xylem hydraulic conductance and outside-xylem hydraulic conductance, as well as correlated traits of vein density, IVD, and intercellular airspace (IAS). There were no correlations between xylem hydraulic conductance, vein density, IVD, and evolutionary age (Figs 3, S5). However, outside-xylem hydraulic conductance and IAS had a significant negative correlation in C_4 grasses (Figs 3, S5).

Lastly, to gain insight into our empirical results, we used our mechanism-based physiological model (Zhou *et al.*, 2018) across varying CO_2 and water-availability environments to consider how variation in hydraulics would affect photosynthesis in C_3 and C_4 grasses. Changing K_{leaf} has a smaller effect on the photosynthesis rate of C_4 than that of C_3 (Fig. 4; Table S27). Decreasing K_{leaf} by half or doubling it changes the photosynthesis rate of a C_4 plant by an average of −4.27% and 3.48%, respectively. By contrast, the same shift in K_{leaf} has average effects of −10.07% and 9.14% on the assimilation rate of a C_3 grass. The sensitivity of the assimilation rate to changes in K_{leaf} decreases with increasing CO_2 concentration and increasing water limitation for both C_3 and C_4 grasses (Table S27), but the assimilation rate of C_4 plants was still less sensitive to K_{leaf} across all permutations of CO_2 concentrations and water availability. These differences in sensitivity to K_{leaf} were robust to differences in physiological properties between C_3 and C_4 (specifically, the temperature response properties and J_{max}/V_{cmax} ratio; Table S3). The

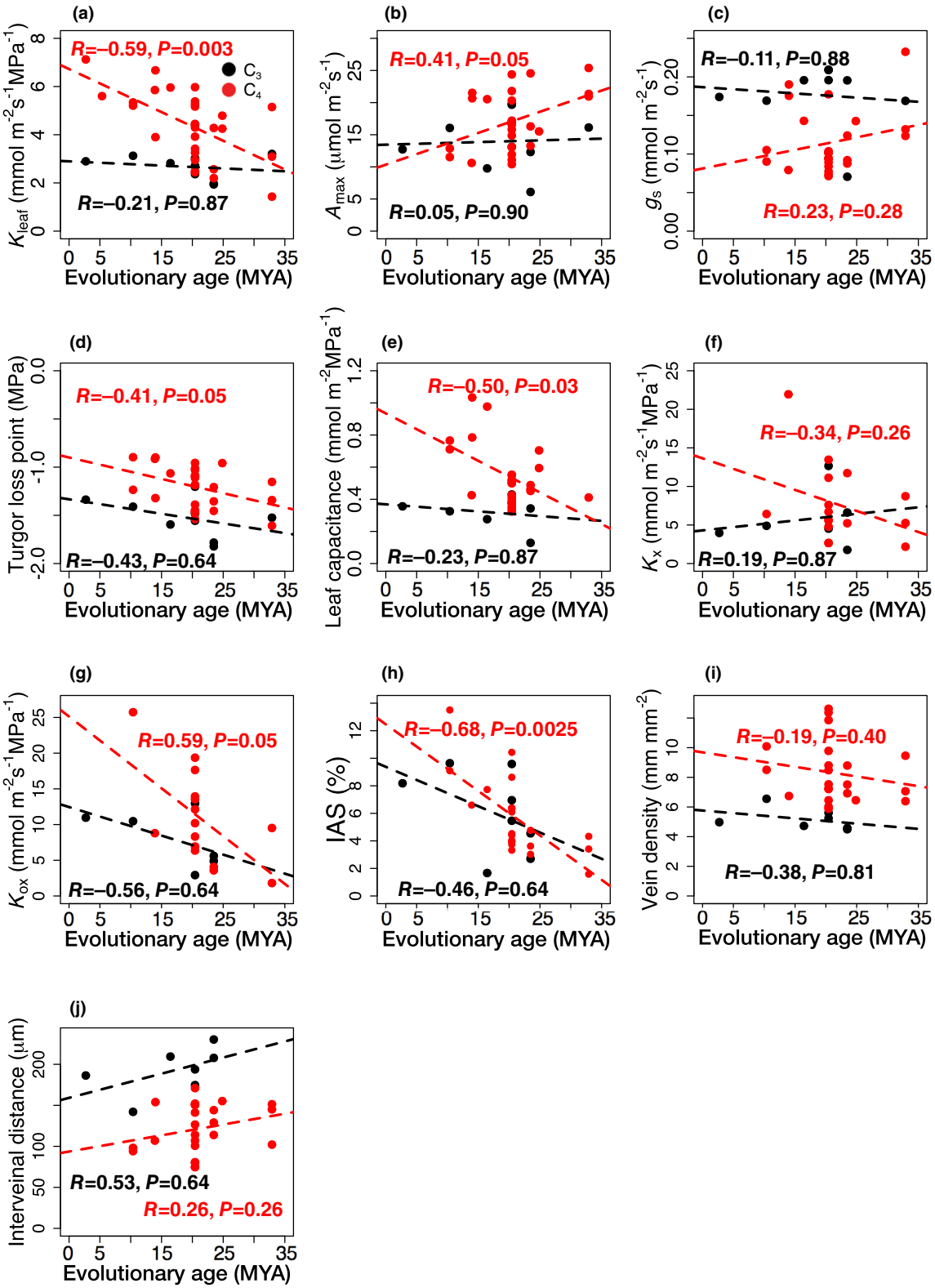

Fig. 3 The regression for hydraulic, anatomical, and photosynthetic traits vs the evolutionary age for the nine origins of C_4 to show an evolutionary trend within C_4 and within their closely related C_3 species. The traits included in the analyses were (a) leaf hydraulic conductance (K_{leaf}), (b) maximal assimilation rate (A_{max}), (c) stomatal conductance (g_s), (d) leaf turgor loss point, (e) leaf capacitance, (f) xylem hydraulic conductance (K_x), (g) outside-xylem hydraulic conductance (K_{ox}), (h) intercellular airspace (IAS), (i) vein density, (j) interveinal distance. The evolutionary age for each sampled origin is derived from the dated phylogeny (Spriggs *et al*., 2014). The intermediate species was not included in our phylogenetic comparative analyses. *P*-values were adjusted using the Benjamini–Hochberg method to control the overall false discovery rate. MYA indicates million years ago.

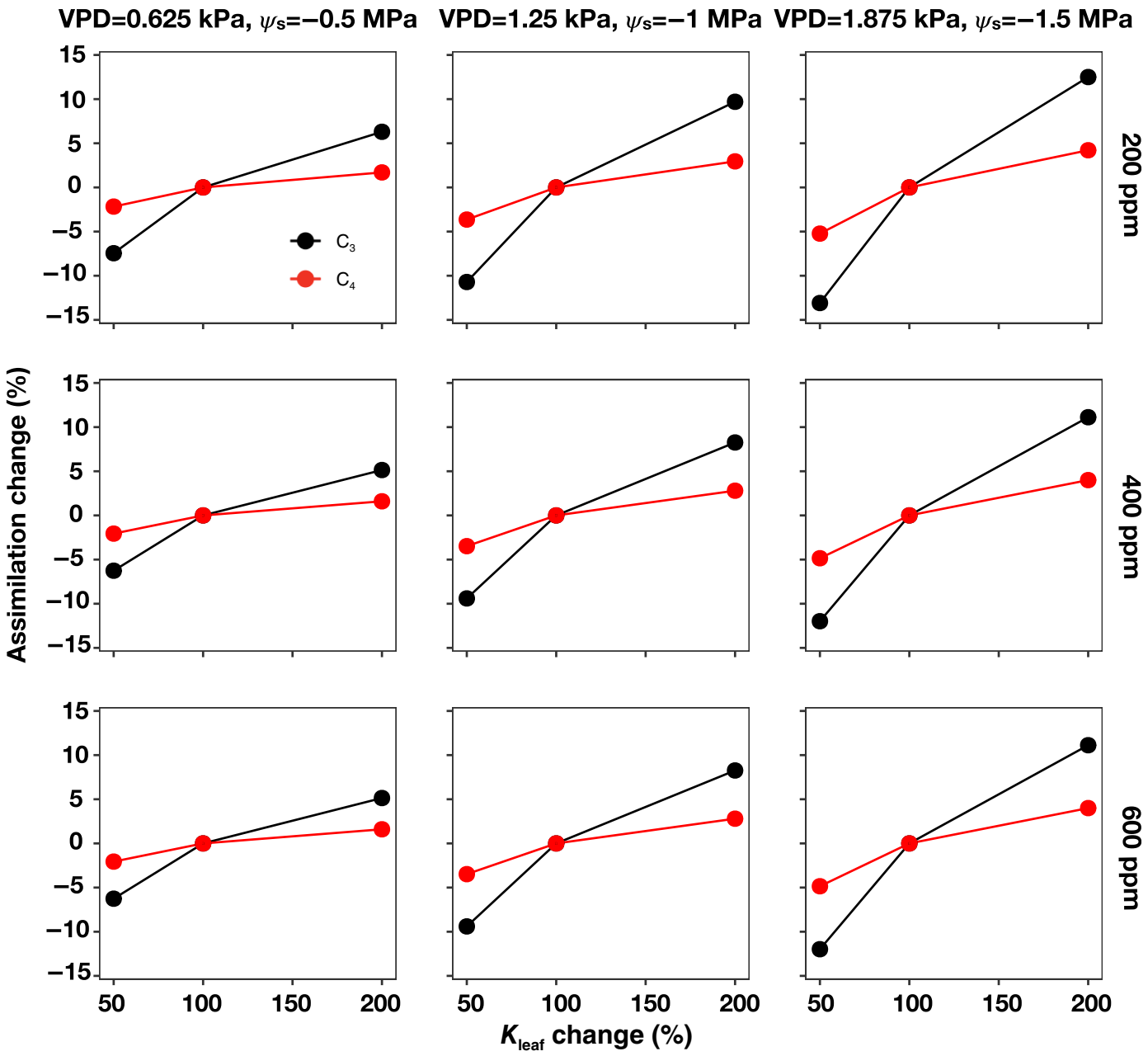

Fig. 4 Modeling results of assimilation rates percentage variation along with leaf hydraulic conductance (K_{leaf}) percentage variation under different CO_2 and water-limited conditions for C_3 (black lines) and C_4 (red lines). C_3 and C_4 parameters are kept the same except for C_4 has the carbon-concentrating mechanism. More simulation results can be found in Supporting Information Table S27. VPD, vapor pressure deficit.

modeling effects of varying K_{leaf} on photosynthesis suggest diminished returns for high-efficiency water transport in C_4 species.

Discussion

The evolution of C_4 photosynthesis in the grasses significantly altered the A_{max}–K_{leaf} relationship, which is thought to operate broadly across vascular plants (Brodribb & Field, 2000; Brodribb *et al.*, 2005, 2007; Fiorin *et al.*, 2016). In addition to other factors (e.g. CO_2, light intensity, and temperature), which were controlled in our experiments, A_{max} can be limited by the efficient transport of water through leaves to replace water loss through open stomata, which is the likely cause of a positive correlation between K_{leaf} and A_{max} across and within plant taxa (Brodribb *et al.*, 2005, 2007; Scoffoni *et al.*, 2016). We found that A_{max} and K_{leaf} are positively correlated in C_3 grasses – supporting previous findings (Brodribb *et al.*, 2007; Scoffoni *et al.*, 2016) – but not in C_4 grasses (Fig. 2). Sonawane *et al.* (2021) and Ocheltree *et al.* (2016) similarly found no relationship between K_{leaf} and A_{max} in C_4 grasses. These studies were not phylogenetically informed, however, and also did not examine C_3 grasses, so the

comparative effect of C_4 evolution on the relationship between K_{leaf} and A_{max} could not be established. To explain the lack of relationship between K_{leaf} and A_{max}, we explore scenarios that are not necessarily mutually exclusive. First, the positive relationship of A_{max} and K_{leaf} is weakened under high K_{leaf}, possibly due to diminished returns of further increasing the efficiency of water transport (Brodribb *et al.*, 2005, 2007), a conclusion supported by our physiological modeling results (Fig. 4). As K_{leaf} tends to be lower in grasses than in other angiosperm species, it is possible that the diminishing returns from increased K_{leaf} manifest at lower values in grasses, and the initial high K_{leaf} resulting from C_4 anatomy could be in the A_{max} 'saturation' zone. Second, we see evidence here that the time-since-C_4-evolution affects several hydraulic traits across and within lineages, and it could be that a walk toward A_{max}–K_{leaf} optimality is slowly occurring within C_4 grass lineages in relatively newfound ecological niches. However, the similar correlations of stomatal conductance vs A_{max} in C_3 and C_4, and lack of evolutionary trend in stomatal conductance, suggest that stomatal conductance might be already near optimal operation or has stabilized faster than supply-side hydraulics. Other hydraulic traits of leaf capacitance and leaf turgor loss point do not seem to contribute to A_{max} directly. The positive correlation between A_{max} and evolutionary age also supports an extended optimization phase for C_4, similar to what was recently found in Bianconi *et al.* (2020). Previous studies have indicated that species from the oldest C_4 lineages (*Chloridoideae* and *Andropogoneae* for example) contain the most productive crops (Sage, 2017), while some recent C_4 lineages are not more productive than C_3 grasses (Ripley *et al.*, 2008; Lundgren *et al.*, 2015). By contrast, the significant decrease in stomatal conductance and the increase in leaf turgor loss point occurred along with the evolution of a fully operational C_4 CCM, as suggested by our physiological models. Consistent with this prediction, in clades that possess a range of C_3, C_3–C_4 intermediate and C_4 physiologies, the increased water use efficiency, decreased stomatal conductance, and a broadened ecological niche are observed only in plants with a full C_4 CCM (Lundgren *et al.*, 2015; Sage *et al.*, 2018).

The evolution of the C_4 pathway in the grasses caused a series of shifts in hydraulic properties when compared to closely related C_3 grasses. Such a conclusion is not easily derived from previous work, as results are often contradictory. Some studies found C_4 species to have significantly higher K_{leaf}, lower stomatal conductance, higher leaf capacitance, and higher leaf turgor loss point/leaf water potential than their closely related C_3 species (Taylor *et al.*, 2010, 2012; Zhou *et al.*, 2018), while other studies found nonsignificantly different or contrasting results for these physiological measures (Taylor *et al.*, 2014; Kocacinar, 2015; Liu & Osborne, 2015; Liu *et al.*, 2019; Sonawane *et al.*, 2021). By examining our data using only ANOVA (Fig. S4), we arrive at similarly contrasting results. How these hydraulic properties compare to C_3 grasses differs based on which C_4 lineage is examined, and no clear pattern emerges. By using phylogenetic comparative analyses, however, a clearer picture emerges indicating that C_4 species had higher K_{leaf}, lower stomatal conductance, higher leaf capacitance, and higher leaf turgor loss points than C_3 grasses when C_4 first evolved. As C_4 species spread and continued to evolve, localized ecophysiological optimization occurred leading to a diversification of C_4 in hydraulic traits. Of particular note here is that turgor loss point is less negative in C_4 grasses in both the phylogenetic models and ANOVA analysis. A more negative turgor loss point is typically indicative of more drought-tolerant plants (Bartlett *et al.*, 2012), yet C_4 grasses tend toward drier sites than C_3 grasses (Pau *et al.*, 2013). While this result seems counterintuitive, the C_4 CCM allows for lower stomatal conductance under drier soil conditions and therefore allows for the maintenance of a less-negative turgor loss point (Zhou *et al.*, 2018). In addition, recent evidence suggests that drought may impact the shuttling of metabolites between bundle sheath cells and mesophyll cells and therefore force C_4 plants to operate at higher turgor loss points (Bellasio *et al.*, 2023).

While it would be ideal if our phylogenetic comparative analyses encompassed a greater representation of the C_4-grass-inclusive PACMAD clade, our results offer compelling yet incomplete evidence of a change in C_4 leaf hydraulics over millions of years; because K_{leaf} and leaf capacitance can be viewed as integrators of whole-leaf hydraulic processes, a potential explanation for this observation is warranted. The high vein density and large bundle sheaths characteristic of C_4 grasses have been predicted to lead to an increase in K_{leaf} and leaf capacitance (Sage, 2001; Griffiths *et al.*, 2012; Osborne & Sack, 2012), and our phylogenetic model results suggest that this occurred the upon the initial evolution of the C_4 CCM. Decreased vein distance and increased bundle sheath size are thought to be anatomical precursors to the evolution of C_4 (Sage, 2004; Christin *et al.*, 2013); therefore, the shifts of K_{leaf} and leaf capacitance likely occurred before, or at the initial formation of, the C_4 CCM.

There are different possible explanations as to why our results show a decline in K_{leaf} over evolutionary time. The first is simply that despite our best efforts in designing the study, the observed pattern may still be influenced by factors such as sampling, biased estimates of evolutionary time, or misspecification of the trait evolution model, among others. The second is that different selective pressures occurred through time as C_4 has evolved in different grass clades. Such a conclusion is supported by the modeling of Zhou *et al.* (2018), where water availability was a stronger selective pressure for lineages that evolved C_4 in the Oligocene and early Miocene. The third possibility is that of a long period of physiological optimization after the initial assembly of a new photosynthetic system. The slow decline in K_{leaf} stands in contrast to the strong initial selection to optimize A_{max} through the coordination of the Calvin–Benson and C_4 cycles within grasses (Zhou *et al.*, 2023). It could be argued that the optimization of traits to increase A_{max} occurred at the expense of K_{leaf}, which is possible only because hydraulic capacity was already 'buffered' by the vein density requirements of C_4, allowing for continued reductions of K_{leaf} at no functional cost.

The apparent change in K_{leaf} over time – which was not accompanied by systematic changes in vein density or xylem conduit diameter – likely occurred via changes in other factors that influence leaf hydraulic capacity, perhaps by the various pathways of water movement between the xylem and the stomatal pores,

and our calculated outside-xylem conductance supports this conclusion (K_{ox} and IAS, Figs 2, 3). Outside-xylem conductance can be affected by the expression of aquaporins, the xylem-to-stomata distance, the organization of internal air spaces and/or the increased suberization of bundle sheath cells (Kocacinar & Sage, 2003; McKown *et al.*, 2010; Scoffoni *et al.*, 2011, 2017; Sonawane *et al.*, 2021), although intercellular air space did indeed decrease with evolutionary time, but it did not correlate with K_{leaf}. Increased suberization of bundle sheath cells is an example of a potential release of an evolutionary constraint: it allows C_4 plants to gain higher A_{max} through reducing bundle sheath leakiness (von Caemmerer & Furbank, 2003; Kromdijk *et al.*, 2014; Wang *et al.*, 2022), but suberization may simultaneously reduce water flow from veins out into the mesophyll. Since C_4 plants are already operating in hydraulic excess, bundle sheath suberization may be optimized for C_4 function without any negative repercussions for plant water relations. This hypothesis could also explain the opposing trends in A_{max} and K_{leaf} when viewed as a function of evolutionary age. Regardless of the mechanism for K_{leaf} decline, the pattern appears to occur independently of lineage in C_4 grasses, does not occur in C_3 grasses, and therefore appears to result from the evolution of the C_4 CCM.

By capitalizing on the multiple origins of C_4 photosynthesis in grasses, we have shown that the vascular organization, which is a hallmark of C_4 plants impacts leaf hydraulics, and disrupts the established link between hydraulic and photosynthetic capacity demonstrated in C_3. The high vein density required to support the photosynthetic CCM leads to C_4 grasses being 'overplumbed' relative to their C_3 counterparts, suggesting that the costs associated with the production of an extensive leaf vasculature require re-evaluation in plants with C_4 photosynthetic systems. The examination of C_4 evolution and hydraulics in grasses therefore provides an exciting system to study both the development of evolutionary constraints and the interplay between photosynthetic and hydraulic physiologies. The phylogenetic-informed experimental design indicated significantly different evolutionary processes in C_3 and C_4 species.

Acknowledgements

HZ was supported by the National Natural Science Foundation of China (42471115). YZ was supported by the Central Guidance on Local Science and Technology Development Funding of Hebei Province (226Z6401G), and the National Natural Science Foundation of China (32071608). BRH was supported by NSF-IOS award 1856587.

Competing interests

None declared.

Author contributions

HZ, EA and BRH contributed to the conceptualization. HZ, EA, EJE, C-LH, AA, YZ and BRH contributed to the methodology and writing – review and editing. HZ and BRH contributed to the investigation. HZ contributed to the visualization. HZ and BRH contributed to the writing – original draft.

ORCID

Erol Akçay https://orcid.org/0000-0001-8149-7124
Erika J. Edwards https://orcid.org/0000-0003-0515-2778
Brent R. Helliker https://orcid.org/0000-0001-7621-2358
Che-Ling Ho https://orcid.org/0000-0002-4354-2438
Haoran Zhou https://orcid.org/0000-0002-5852-9535

Data availability

All the data for this paper could be found in the main text and Supporting Information (Figs S4, S5; Tables S4, S27).

References

Akaike H. 1974. A new look at the statistical model identification. *IEEE Transactions on Automatic Control* **19**: 716–723.

Bartlett MK, Scoffoni C, Sack L. 2012. The determinants of leaf turgor loss point and prediction of drought tolerance of species and biomes: a global meta-analysis. *Ecology Letters* **15**: 393–405.

Bellasio C, Stuart-Williams H, Farquhar GD, Flexas J. 2023. C_4 maize and sorghum are more sensitive to rapid dehydration than C_3 wheat and sunflower. *New Phytologist* **240**: 2239–2252.

Bianconi ME, Hackel J, Vorontsova MS, Alberti A, Arthan W, Burke SV, Duvall MR, Kellogg EA, Lavergne S, McKain MR *et al.* 2020. Continued adaptation of C_4 photosynthesis after an initial burst of changes in the andropogoneae grasses. *Systematic Biology* **69**: 445–461.

Brodribb TJ, Field TS. 2000. Stem hydraulic supply is linked to leaf photosynthetic capacity: evidence from New Caledonian and Tasmanian rainforests. *Plant, Cell & Environment* **23**: 1381–1388.

Brodribb TJ, Field TS, Jordan GJ. 2007. Leaf maximum photosynthetic rate and venation are linked by hydraulics. *Plant Physiology* **144**: 1890–1898.

Brodribb TJ, Holbrook NM, Zwieniecki MA, Palma B. 2005. Leaf hydraulic capacity in ferns, conifers and angiosperms: impacts on photosynthetic maxima. *New Phytologist* **165**: 839–846.

Burnham KP, Anderson DR. 1998. Practical use of the information-theoretic approach. In: Burnham KP, Anderson DR, eds. *Model selection and inference.* New York, NY, USA: Springer, 75–117.

von Caemmerer S, Furbank RT. 2003. The C_4 pathway: an efficient CO_2 pump. *Photosynthesis Research* **77**: 191–207.

Cavanaugh JE. 1997. Unifying the derivations for the Akaike and corrected Akaike information criteria. *Statistics & Probability Letters* **33**: 201–208.

Christin PA, Osborne CP, Chatelet DS, Columbus JT, Besnard G, Hodkinson TR, Garrison LM, Vorontsova MS, Edwards EJ. 2013. Anatomical enablers and the evolution of C_4 photosynthesis in grasses. *Proceedings of the National Academy of Sciences, USA* **110**: 1381–1386.

Clavel J, Escarguel G, Merceron G. 2015. MVMORPH: an R package for fitting multivariate evolutionary models to morphometric data. *Methods in Ecology and Evolution* **6**: 1311–1319.

Donnelly RC, Wedel ER, Taylor JH, Nippert JB, Helliker BR, Riley WJ, Still CJ, Griffith DM. 2023. Evolutionary lineage explains trait variation among 75 coexisting grass species. *New Phytologist* **239**: 875–887.

Edwards EJ. 2019. Evolutionary trajectories, accessibility and other metaphors: the case of C_4 and CAM photosynthesis. *New Phytologist* **223**: 1742–1755.

Edwards EJ, Smith SA. 2010. Phylogenetic analyses reveal the shady history of C_4 grasses. *Proceedings of the National Academy of Sciences, USA* **107**: 2532–2537.

Edwards EJ, Still CJ. 2008. Climate, phylogeny and the ecological distribution of C_4 grasses. *Ecology Letters* **11**: 266–276.

Ehleringer JR, Cerling TE, Helliker BR. 1997. C_4 photosynthesis, atmospheric CO_2, and climate. *Oecologia* **112**: 285–299.

Ehleringer JR, Monson RK. 1993. Evolutionary and ecological aspects of photosynthesis pathway variation. *Annual Review of Ecology and Systematics* **24**: 411–439.

Fiorin L, Brodribb TJ, Anfodillo T. 2016. Transport efficiency through uniformity: organization of veins and stomata in angiosperm leaves. *New Phytologist* **209**: 216–227.

Grass Phylogeny Working Group II (GPWGII). 2012. New grass phylogeny resolves deep evolutionary relationships and discovers C_4 origins. *New Phytologist* **193**: 304–312.

Griffiths H, Weller G, Toy L, Dennis RJ. 2012. You're so vein: bundle sheath physiology, phylogeny and evolution in C_3 and C_4 plants. *Plant, Cell & Environment* **36**: 249–261.

Hamim H, Banon S, Dorly D. 2016. Comparison of physiological and anatomical changes of C_3 (*Oryza sativa* [L.]) and C_4 (*Echinochloa crusgalli* [L.]) leaves in response to drought stress. *IOP Conference Series: Earth and Environmental Science* **31**: 12040.

Heyduk K, Moreno-Villena JJ, Gilman IS, Christin PA, Edwards EJ. 2019. The genetics of convergent evolution: insights from plant photosynthesis. *Nature Reviews. Genetics* **20**: 485–493.

Huxman TE, Monson RK. 2003. Stomatal responses of C_3, C_3–C_4 and C_4 Flaveria species to light and intercellular CO_2 concentration: implications for the evolution of stomatal behaviour. *Plant, Cell & Environment* **26**: 313–322.

Kocacinar F. 2015. Photosynthetic, hydraulic and biomass properties in closely related C_3 and C_4 species. *Physiologia Plantarum* **153**: 454–466.

Kocacinar F, Sage RF. 2003. Photosynthetic pathway alters xylem structure and hydraulic function in herbaceous plants. *Plant, Cell & Environment* **26**: 2015–2026.

Kromdijk J, Ubierna N, Cousins AB, Griffiths H. 2014. Bundle-sheath leakiness in C_4 photosynthesis: a careful balancing act between CO_2 concentration and assimilation. *Journal of Experimental Botany* **65**: 3443–3457.

Leakey AD, Ferguson JN, Pignon CP, Wu A, Jin Z, Hammer GL, Lobell DB. 2019. Water use efficiency as a constraint and target for improving the resilience and productivity of C_3 and C_4 crops. *Annual Review of Plant Biology* **70**: 781–808.

Lewis AM. 1992. Measuring the hydraulic diameter of a pore or conduit. *American Journal of Botany* **79**: 1158–1161.

Lewis AM, Boose ER. 1995. Estimating volume flow rates through xylem conduits. *American Journal of Botany* **82**: 1112–1116.

Liu H, Osborne CP. 2015. Water relations traits of C_4 grasses depend on phylogenetic lineage, photosynthetic pathway, and habitat water availability. *Journal of Experimental Botany* **66**: 761–773.

Liu H, Taylor SH, Xu Q, Lin Y, Hou H, Wu G, Ye Q. 2019. Life history is a key factor explaining functional trait diversity among subtropical grasses, and its influence differs between C_3 and C_4 species. *Journal of Experimental Botany* **70**: 1567–1580.

Lundgren MR, Besnard G, Ripley BS, Lehmann CE, Chatelet DS, Kynast RG, Namaganda M, Vorontsova MS, Hall RC, Elia J *et al.* 2015. Photosynthetic innovation broadens the niche within a single species. *Ecology Letters* **18**: 1021–1029.

Males J, Griffiths H. 2018. Economic and hydraulic divergences underpin ecological differentiation in the Bromeliaceae. *Plant, Cell & Environment* **41**: 64–78.

Marshall B, Biscoe PV. 1980. A model for C_3 leaves describing the dependence of net photosynthesis on irradiance. *Journal of Experimental Botany* **31**: 29–39.

McKown AD, Cochard H, Sack L. 2010. Decoding leaf hydraulics with a spatially explicit model: principles of venation architecture and implications for its evolution. *The American Naturalist* **175**: 447–460.

North GB, Lynch FH, Maharaj FDR, Phillips CA, Woodside WT. 2013. Leaf hydraulic conductance for a tank bromeliad: axial and radial pathways for moving and conserving water. *Frontiers in Plant Science* **4**: 78.

Ocheltree TW, Nippert JB, Prasad PV. 2014. Stomatal sensitivity of C_3 and C_4 grasses. *Plant, Cell & Environment* **37**: 132–139.

Ocheltree TW, Nippert JB, Prasad PV. 2016. A safety vs efficiency trade-off identified in the hydraulic pathway of grass leaves is decoupled from photosynthesis, stomatal conductance and precipitation. *New Phytologist* **210**: 97–107.

Osborne CP, Sack L. 2012. Evolution of C_4 plants: a new hypothesis for an interaction of CO_2 and water relations mediated by plant hydraulics. *Philosophical Transactions of the Royal Society of London. Series B: Biological Sciences* **367**: 583–600.

Pathare VS, Sonawane BV, Koteyeva N, Cousins AB. 2020. C_4 grasses adapted to low precipitation habitats show traits related to greater mesophyll conductance and lower leaf hydraulic conductance. *Plant, Cell & Environment* **43**: 1897–1910.

Pau S, Edwards EJ, Still CJ. 2013. Improving our understanding of environmental controls on the distribution of C_3 and C_4 grasses. *Global Change Biology* **19**: 184–196.

Pearcy RW, Ehleringer JR. 1984. Comparative ecophysiology of C_3 and C_4 plants. *Plant, Cell & Environment* **7**: 1–13.

Ripley BS, Abraham TI, Osborne CP. 2008. Consequences of C_4 photosynthesis for the partitioning of growth: a test using C_3 and C_4 subspecies of *Alloteropsis semialata* under nitrogen-limitation. *Journal of Experimental Botany* **59**: 1705–1714.

Sack L, Cowan PD, Jaikumaar N, Holbrook NM. 2003. The 'hydrology' of leaves: co-ordination of structure and function in temperate woody species. *Plant, Cell & Environment* **26**: 1343–1356.

Sack L, Frole K. 2006. Leaf structural diversity is related to hydraulic capacity in tropical rain forest trees. *Ecology* **87**: 483–491.

Sack L, Holbrook NM. 2006. Leaf hydraulics. *Annual Review of Plant Biology* **57**: 361–381.

Sack L, Pasquet-Kok J, PrometheusWiki Contributors. 2010. Leaf pressure-volume curve parameters. PrometheusWiki. May 20, 2010, 17:08 UTC. [WWW document] URL http://www.publish.csiro.au/prometheuswiki/tiki-pagehistory.php?page=Leafpressure-volumecurveparameters&preview=16 [accessed 11 March 2016].

Sack L, Scoffoni C. 2012. Measurement of leaf hydraulic conductance and stomatal conductance and their responses to irradiance and dehydration using the Evaporative Flux Method (EFM). *Journal of Visualized Experiments* **70**: e4179.

Sage RF. 2001. Environmental and evolutionary preconditions for the origin and diversification of the C_4 photosynthetic syndrome. *Plant Biology* **3**: 202–213.

Sage RF. 2004. The evolution of C_4 photosynthesis. *New Phytologist* **161**: 341–370.

Sage RF. 2017. A portrait of the C_4 photosynthetic family on the 50th anniversary of its discovery: species number, evolutionary lineages, and Hall of Fame. *Journal of Experimental Botany* **68**: e11–e28.

Sage RF, Monson RK, Ehleringer JR, Adachi S, Pearcy RW. 2018. Some like it hot: the physiological ecology of C_4 plant evolution. *Oecologia* **187**: 941–966.

Sage RF, Sage TL, Kocacinar F. 2012. Photorespiration and the evolution of C_4 photosynthesis. *Annual Review of Plant Biology* **63**: 19–47.

Schindelin J, Arganda-Carreras I, Frise E, Kaynig V, Longair M, Pietzsch T, Cardona A. 2012. Fiji: an open-source platform for biological-image analysis. *Nature Methods* **9**: 676–682.

Schlüter U, Weber AP. 2020. Regulation and evolution of C_4 photosynthesis. *Annual Review of Plant Biology* **71**: 183–215.

Scoffoni C, Albuquerque C, Brodersen CR, Townes SV, John GP, Bartlett MK, Buckley TN, McElrone AJ, Sack L. 2017. Outside-xylem vulnerability, not xylem embolism, controls leaf hydraulic decline during dehydration. *Plant Physiology* **173**: 1197–1210.

Scoffoni C, Chatelet DS, Pasquet-kok J, Rawls M, Donoghue MJ, Edwards EJ, Sack L. 2016. Hydraulic basis for the evolution of photosynthetic productivity. *Nature Plants* **2**: 16072.

Scoffoni C, Rawls M, Mckown A, Cochard H, Sack L. 2011. Decline of leaf hydraulic conductance with dehydration: relationship to leaf size and venation architecture. *Plant Physiology* **156**: 832–843.

Smith JAC, Heuer SS. 1981. Determination of the volume of intercellular spaces in leaves and some values for CAM plants. *Annals of Botany* **48**: 915–917.

Sonawane BV, Koteyeva NK, Johnson DM, Cousins AB. 2021. Differences in leaf anatomy determines temperature response of leaf hydraulic and mesophyll CO_2 conductance in phylogenetically related C_4 and C_3 grass species. *New Phytologist* **230**: 1802–1814.

Spriggs EL, Christin PA, Edwards EJ. 2014. C_4 photosynthesis promoted species diversification during the Miocene grassland expansion. *PLoS ONE* **9**: e97722.

Stiller V, Lafitte HR, Sperry JS. 2003. Hydraulic properties of rice and the response of gas exchange to water stress. *Plant Physiology* **132**: 1698–1706.

Taylor SH, Franks PJ, Hulme SP, Spriggs E, Christin PA, Edwards EJ, Woodward FI, Osborne CP. 2012. Photosynthetic pathway and ecological adaptation explain stomatal trait diversity amongst grasses. *New Phytologist* **193**: 387–396.

Taylor SH, Hulme SP, Rees M, Ripley BS, Woodward FI, Osborne CP. 2010. Ecophysiological traits in C_3 and C_4 grasses: a phylogenetically controlled screening experiment. *New Phytologist* **185**: 780–791.

Taylor SH, Ripley BS, Martin T, De-Wet LA, Woodward FI, Osborne CP. 2014. Physiological advantages of C_4 grasses in the field: a comparative experiment demonstrating the importance of drought. *Global Change Biology* **20**: 1922–2003.

Tyree MT, Hammel HT. 1972. The measurement of the turgor pressure and the water relations of plants by the pressure-bomb technique. *Journal of Experimental Botany* **23**: 267–282.

Ueno O, Kawano Y, Wakayama M, Takeda T. 2006. Leaf vascular systems in C_3 and C_4 grasses: a two-dimensional analysis. *Annals of Botany* **97**: 611–621.

Vadez V, Choudhary S, Kholova J, Hash CT, Srivastava R, Kumar AA, Prandavada A, Anjaiah M. 2021. Transpiration efficiency: further insights from C_4 cereals species comparison. *Journal of Experimental Botany* **72**: 5221–5234.

Wang Y, Stutz SS, Bernacchi CJ, Boyd RA, Ort DR, Long SP. 2022. Increased bundle-sheath leakiness of CO_2 during photosynthetic induction shows a lack of coordination between the C_4 and C_3 cycles. *New Phytologist* **236**: 1661–1675.

Way DA, Katul GG, Manzoni S, Vico G. 2014. Increasing water use efficiency along the C_3 to C_4 evolutionary pathway: a stomatal optimization perspective. *Journal of Experimental Botany* **65**: 3683–3693.

Wolfe B, Detto M, Zhang YJ, Anderson-Teixeira KJ, Brodribb T, Collins AD, Crawford C, Dickman LT *et al.* 2022. Leaves as bottlenecks: the contribution of tree leaves to hydraulic resistance within the soil-plant-atmosphere continuum. *Plant, Cell & Environment* **46**(3): 736–746.

Zhou H, Akçay E, Helliker B. 2023. Optimal coordination and reorganization of photosynthetic properties in C4 grasses. *Plant, Cell & Environment* **46**: 796–811.

Zhou H, Helliker BR, Huber M, Dicks A, Akçay E. 2018. C_4 photosynthesis and climate through the lens of optimality. *Proceedings of the National Academy of Sciences, USA* **115**: 12057–12062.

Supporting Information

Additional Supporting Information may be found online in the Supporting Information section at the end of the article.

Fig. S1 Dated phylogeny of our species in the current study for phylogenetic analysis.

Fig. S2 Nondated phylogeny of our species in the current study for phylogenetic analysis.

Fig. S3 Comparisons of modeled K_x from anatomical measurements to measured K_x for five species.

Fig. S4 Color bar plot of hydraulic and photosynthetic traits for each of the targeted C_3 and C_4 species.

Fig. S5 Evolutionary trends for the hydraulic traits (K_{leaf}, leaf capacitance, leaf turgor loss point, g_s, K_x, K_{ox}), photosynthetic traits (A_{max}), anatomical traits (vein density, interveinal distance, IAS), and $\delta^{13}C$ with the evolutionary branch length from a nondated phylogenetic tree.

Methods S1 Phylogenetic comparative analysis.

Notes S1 Results and discussion.

Table S1 Percentage difference between reference CO_2 and sample CO_2 in the measurements of the light curve.

Table S2 The evolutionary models used for the phylogenetic analysis.

Table S3 Description of evolutionary models to be fitted for C_3 and C_4 subtype species.

Table S4 Input physiological parameters used for C_3 and C_4 modeling.

Table S5 Phylogenetic analysis results for hydraulic conductance (K_{leaf}) for C_3 and C_4 species.

Table S6 Phylogenetic analysis results for leaf capacitance for C_3 and C_4 species.

Table S7 Phylogenetic analysis results for stomatal conductance (g_s) for C_3 and C_4 species.

Table S8 Phylogenetic analysis results for leaf turgor loss point (Turgor loss) for C_3 and C_4 species.

Table S9 Phylogenetic analysis results for A_{max} for C_3 and C_4 species.

Table S10 Phylogenetic analysis results of best-fitted models considering the C_4 subtype for K_{leaf}, leaf capacitance, g_s, and leaf turgor loss point.

Table S11 Estimated correlation between A_{max} and K_{leaf} for C_3 and C_4.

Table S12 Estimated correlation between A_{max} and leaf capacitance for C_3 and C_4.

Table S13 Estimated correlation between A_{max} and g_s for C_3 and C_4.

Table S14 Estimated correlation between A_{max} and leaf turgor loss for C_3 and C_4.

Table S15 Estimated correlation between A_{max} and bundle sheath size for C_3 and C_4.

Table S16 Estimated correlation between K_{leaf} and vein density for C_3 and C_4.

Table S17 Estimated correlation between K_{leaf} and interveinal distance for C_3 and C_4.

Table S18 Estimated correlation between K_{leaf} and intercellular airspace (IAS) for C_3 and C_4.

Table S19 Estimated correlation between K_{leaf} and conduit diameter for C_3 and C_4.

Table S20 Estimated correlation between K_{leaf} and bundle sheath size for C_3 and C_4.

Table S21 Phylogenetic results of the best-fitted models and their parameters using models from Table S2 and the nondated phylogenetic tree (summarizing Tables S22–S26).

Table S22 Phylogenetic analysis results for hydraulic conductance (K_{leaf}) for C_3 and C_4 species.

Table S23 Phylogenetic analysis results for leaf capacitance for C_3 and C_4 species.

Table S24 Phylogenetic analysis results for stomatal conductance (g_s) for C_3 and C_4 species.

Table S25 Phylogenetic analysis results for leaf turgor loss point (Turgor loss) for C_3 and C_4 species.

Table S26 Phylogenetic analysis results for A_{max} for C_3 and C_4 species.

Table S27 Modeling results about the effects of varying hydraulic conductance on the assimilation rates under different water-limited conditions and CO_2 concentrations.

Please note: Wiley is not responsible for the content or functionality of any Supporting Information supplied by the authors. Any queries (other than missing material) should be directed to the *New Phytologist* Central Office.